Synoptic airborne thickness surveys reveal state of Arctic sea ice cover

Christian Haas[1], Stefan Hendricks[2], Hajo Eicken[3], Andreas Herber[2]

[1] University of Alberta, Edmonton, Canada

[2] Alfred Wegener Institute for Polar and Marine Research, Bremerhaven, Germany

[3] University of Alaska, Fairbanks, USA

Abstract

While summer Arctic sea-ice extent has decreased over the past three decades, it is subject to large interannual and regional variations. Methodological challenges in measuring ice thickness continue to hamper our understanding of the response of the ice-thickness distribution to recent change, limiting the ability to forecast sea-ice change over the next decade. We present results from a 2400 km long pan-Arctic airborne electromagnetic (EM) ice thickness survey in April 2009, the first-ever large-scale EM thickness dataset obtained by fixed-wing aircraft over key regions of old ice in the Arctic Ocean between Svalbard and Alaska. The data provide detailed insight into ice thickness distributions characteristic for the different regions. Comparison with previous EM surveys shows that modal thicknesses of old ice had changed little since 2007, and remained within the expected range of natural variability.

Introduction

Over the last 30 years, the areal extent of summer Arctic sea ice has rapidly declined at a rate of 11.2%/decade. It plummeted to a record minimum coverage of 4.28×10^6 km^2 in September 2007, with only slightly higher extent in 2008. However, as sea ice is subject to strong interannual variability [*Haas and Eicken*, 2001], ice extent in 2009 was higher, and with 5.36×10^6 km^2 close to the multidecadal linear trend. Sea-ice thinning and retreat are expected to continue as a result of climate change, amplified by ice-albedo feedback. There is evidence from model simulations that Arctic sea ice is in a transition to long-term reductions and eventual loss of summer ice [*Holland et al.,* 2006; *Lindsay and Zhang*, 2005]. However, discussions among scientists contributing to a community-wide sea-ice outlook in summer of 2008 and 2009, highlighted the dominant role that weather and large-scale atmospheric circulation play in either compounding or compensating the preconditioning effects of climate change on the state of the ice cover [*Overland et al.,* 2009; *SEARCH Sea Ice Outlook*, unpublished, 2009]. The Outlook also established that more reliable forecasts of ice evolution over the course of the summer require improved ice thickness information to help evaluate the initial state of the ice cover before the onset of summer melt.

However, accurate ice thickness information is still scarce over wide regions of the Arctic Ocean. Most ice thickness data over the past few decades have been obtained during sporadic nuclear submarine cruises, by means of upward-looking echo-sounders capable of measuring the draft of ice floes [*Wadhams and Davis*, 2001; *Rothrock and Wensnahan*, 2007]. Significant advances have furthered retrieval of ice thickness from freeboard (here:

height of the ice or snow surface above the water level) measurements by airborne and satellite radar and laser altimetry [*Hvidegaard and Forsberg*, 2002; *Giles et al.,* 2007; *Kwok and Cunningham*, 2008]. Similar to submarine draft measurements, ice thickness can be computed from freeboard based on assumptions about the ice density profile and snow density and depth [*Kwok and Cunningham*, 2008]. However, since the freeboard/thickness ratio is much smaller than the draft/thickness ratio, uncertainties in the freeboard retrieval and in snow density and depth result in much larger errors of the obtained ice thicknesses. While recent results hold promise, a detailed validation of altimetry measurements is still pending. *Kwok et al.* [2009] showed that basin-wide Arctic sea-ice volume strongly decreased between 2003 and 2008, mostly due to replacement of multiyear by first-year ice as a result of recent regime shifts [*Maslanik et al.,* 2007; *Nghiem et al.,* 2007], and thinning of multiyear ice. However, they did not observe significant changes in the mean thickness of the first-year ice regions.

Electromagnetic induction (EM) sounding allows for surveys of total (ice-plus-snow) sea-ice thickness utilizing the strong electrical conductivity contrast between ice and seawater. Snow depth uncertainties have less impact on the accuracy of the ice thickness retrieval than with altimetry. Ground and helicopter-borne EM surveys have shown that the modal thickness of second-and multiyear ice in the region of the North Pole has decreased by 0.9 m between 1991 and 2007 [*Haas et al.,* 2008]. Modal thickness at the North Pole plummeted from 2.2 m in 2004 to 0.9 m in the summer of 2007, mainly as a result of first-year ice replacing old ice [*Haas et al.,* 2008].

Here, we present results of an extensive synoptic airborne EM ice thickness survey, carried out in April 2009, over key regions of the Arctic Ocean north of Svalbard, Greenland, Canada, and Alaska, predominantly covered by multiyear ice (Figure 1). This survey was performed to assess the present state of the Arctic sea ice cover, to validate satellite data, for comparison with observations from previous years, and to provide background information for the prediction and interpretation of sea ice changes in the summer of 2009 and subsequent years. As previous helicopter-borne surveys were severely range-limited and logistically involved (e.g. Haas et al., 2006), we have for the first time developed a towed EM system for a fixed-wing aircraft (Figure 2).

Measurements

EM sounding is a classical geophysical method to detect the distance between an EM instrument and the boundary between the resistive sea ice and the conductive sea water, i.e. its altitude above the ice/water-interface [*Kovacs et al.,* 1987]. The method is based on measurements of the amplitude and phase of a secondary EM field induced in the seawater by a primary field transmitted by the EM instrument. Surveys are usually performed with a towed sensor package ("EM Bird"), which is operated some tens of meters below the aircraft, and 20 m above the ice. The Bird's altitude above the snow or ice surface is measured with a laser altimeter. Ice-plus-snow thickness (hereafter referred to as ice thickness) results from the difference between the altitude above the ice/water-interface and above the snow or ice surface [*Haas et al.,* 2009].

The accuracy of EM measurements is ±0.1 m over level ice [*Pfaffling et al.,* 2007; *Haas et al.*, 2009]. However, the maximum thickness of pressure ridges is generally underestimated due to their porosity and the EM footprint diameter of up to 3.7 times the instrument altitude [*Reid et al.,* 2006]. The measured thickness of unconsolidated ridges can be less than 50% of the "true" thickness [e.g., *Haas and Jochmann*, 2003]. Therefore, obtained thickness distributions are most accurate with respect to their modal thickness, while mean ice thickness can still be used for relative comparisons between regions and campaigns.

Operation of a towed bird is advantageous because this eliminates electromagnetic induction in metal parts of the towing aircraft. Also, towing of birds allows their operation closer to the ice and water surface, were the EM field induced in the water is strongest and higher signal-to-noise ratios can be achieved. Here, we operated an EM Bird under a Basler BT-67 fixed-wing aircraft, a rebuilt and modernized DC-3 (Figure 2). The plane is ideally suited for operation of an EM Bird, which can be cradled under the fuselage for take-off and landing (Figure 2), and is lowered with a winch for surveying. For the 2009 surveys, the Bird was operated with an 80 m long tow cable 20 m above the ice surface, such that the plane could fly at a height of 100 m above the ice, and with a speed of 120 knots. A downward-looking video camera showed that Bird swaying and rolling was less than with helicopters, owing to larger drag on the longer tow cable. The plane was also less affected by turbulence and altitude variations than a helicopter. Measurements were performed with a point spacing of approximately 5 m.

Ice thickness surveys were performed as part of the Pan-Arctic Measurements and Arctic Regional Climate Model Simulations project (PAM-ARCMIP). In addition to ice thickness,

measurements of aerosols, trace gases, cloud distributions, as well as meteorological and atmospheric conditions were performed over the same regions. As flying time and payload capacity had to be shared between the different activities, ice thickness surveys were mostly limited to lengths of less than 500 km and could only be made during either the outward or inward leg of each flight, because the other leg was flown at altitudes of more than 3300 m. All surveys were performed between April 5, when the campaign commenced in Longyearbyen (Svalbard, Norway), and April 26, when it ended in Barrow (Alaska; Figure 1). Station Nord (Greenland), Canadian Forces Station Alert (Ellesmere Island, Nunavut), the Russian drifting station NP-36 close to the North Pole, Eureka (Ellesmere Island, Nunavut), Resolute Bay (Cornwallis Island, Nunavut), and Sachs Harbor (Banks Island, Northwest Territories) were used as bases for re-fuelling or overnighting. Due to weather conditions, surveys could only be flown from Longyearbyen, Alert, Sachs Harbour, and Barrow (Figure 1).

Results and discussion

Figure 1 shows the locations of all 9 survey flights, with a total length of 2412 km. Radar backscatter obtained by the QuikSCAT Ku-band scatterometer indicates the distribution of first-year and multiyear ice with low and high backscatter, respectively [*Nghiem et al.,* 2007]. The flight tracks covered the expanses of multiyear ice between Ellesmere Island and the North Pole (Flights 3-5), as well as the main outflow branches of old ice from the Arctic Ocean through Fram Strait (Flights 1 & 2) and into the Beaufort and Chukchi Seas (Flights 6-9).

The thickest ice with mean thicknesses of up to 6.06 m (averaged along 20-km segments, Figure 1, see also Table 1) was found along the coast of Ellesmere Island (Flights 3, 4, and 5) as a result of deformation driven by shoreward ice motion. The thinnest ice with mean thicknesses between 1.69 m and 1.88 m was surveyed in the Beaufort and Chukchi Seas and in Fram Strait. Note that ice thicknesses in these regions were very similar. Most flights showed significant thickening from South to North, primarily due to the larger fractions of older ice further north [*Maslanik et al.,* 2007] and reduced summer bottom and surface ablation [*Perovich et al.,* 2008]. Along the Ellesmere Island - North Pole transect ice thickness decreased due to prevalence of younger, less deformed ice further north.

The ice thickness distribution histograms shown in Figure 1 provide much better insight into the state of the sea ice cover than mean values. The modes apparent in the distributions correspond to new ice, level first-year, and level older ice (Table 1). In Fram Strait, strongly bimodal distributions reflect the divergent nature of the outflowing ice pack, with large leads covered by new ice. In contrast, the convergent ice regimes north of Greenland and Ellesmere Island lack new ice or open water, with few patches of first-year ice 1.8 to 2 m thick. Distributions exhibit broad modes between 3.1 and 4.5 m thick, and long, exponential tails representing large fractions of pressure ridges frequently thicker than 10 m.

To assess variability and change in the aftermath of the 2007 record ice minimum, comparisons with data from prior, more localized EM overflights in three regions are instructive (Figure 3, Table 2). Modal thickness increased from 2.4 to 2.8 m at the North Pole, despite a decrease in the amount of ridged ice that is responsible for a smaller mean

thickness. North of Ellesmere Island modal thicknesses recovered to 4.3 m, with as extensive ridging as in past years and less young ice (Haas et al., 2006). We expect little change between thicknesses in April and May used in this comparison, as this is at the end of the winter and because the ice was already very thick. This increase follows a drastic decline observed in 2008, which is in agreement with results by *Giles et al.* [2008], and *Kwok et al.* [2009] , and was likely due to high ablation in the summer of 2007 [*Perovich et al.,* 2008] and reduced deformation due to anomalous, winter-long southward export of ice through Nares Strait between Ellesmere Island and Greenland.

Flight 6 off Banks Island sampled the core of the drift stream of multiyear ice advected from north of the High Canadian Arctic. However, the areal fraction of multiyear ice in the western Beaufort and Chukchi Seas was significantly reduced following the 2007 ice minimum, as indicated by Flight 8 and QuikSCAT data, dominated by low-backscatter ice in this region (Figure 1). In 2009, multiyear ice was too rare to result in any mode. In the Chukchi Sea, the modal thickness of first-year ice was near-constant between 2007 and 2009.

Conclusions

We conclude that older sea ice in much of the Arctic Ocean was of similar or even slightly larger thickness in April 2009 relative to conditions in 2007, but within the expected range of interannual variability. However, the volume of older ice may have been less overall due to a lower areal coverage, and because our surveys were still spatially limited. It seems that consequences of strong melt and ice export during and after the summer record minimum 2007 may have been compensated for by weather patterns in 2008 that were not conducive to high melt and ice dispersal in summer and may have fostered enhanced thermodynamic ice growth during a colder winter 2008/09 with less snow accumulation, as suggested by anecdotal in-situ observations in spring 2009 [*SEARCH Sea Ice Outlook*, unpublished, 2009; *CATLIN Arctic Survey*, unpublished, 2009]. A key finding of the 2009 EM surveys is that with mostly unchanged first-year level ice thickness modes, much hinges on the thickening through deformation and thinning through melt and export in assessing the resilience of the Arctic ice pack towards further reductions in extent and thickness. The balance between high melt rates and import of old ice into the Beaufort and Chukchi Seas will be an important variable in determining potential recovery or further Arctic ice mass loss [*Barber et al*., 2009]. The present study goes a long way toward establishing fixed-wing airborne EM surveys as an ideal complement to the strengths and weaknesses of other operational ice thickness measurement methods. It provides near-real-time data of the marginal seas and shallow shelf areas of the Arctic Ocean where submarine data cannot be acquired or disclosed, and allows a more detailed dissection of thickness distributions with secondary and tertiary modes than possible with satellite altimetry due to its smaller

footprint. An Arctic sea-ice observation system combining all three methods is of particular value in addressing significant shortcomings in data coverage and accuracy needed to improve the blending of model output and observational data in tracking and forecasting the mass-balance of the Arctic ice cover on seasonal to decadal timescales. The fixed-wing towed EM system will be extensively used during upcoming CryoSat validation campaigns planned for April 2011 and 2012 between Canada and the North Pole.

Acknowledgement

We thank Environment Canada (Toronto, Canada), the Arctic and Antarctic Research Institute (St. Petersburg, Russia), and the National Oceanographic and Atmospheric Administration (Boulder, USA) for their great logistical support. Pioneering engineering by Jim Hodgson, Elton Townsend (Lake Central Air Service, Bracebridge, Canada), John Lobach (Ferra Dynamics Inc., Mississauga, Canada), and Martin Gehrmann and Manuel Sellman (AWI, Germany) implementing the winch and bird systems is greatly acknowledged. Brian Burchartz and Andrew Jenkins of Enterprise Airlines Inc. (Oshawa, Canada) are thanked for their highly demanding flying. Other data presented in this paper were obtained through the EU-funded GreenICE and NSF-funded SIZONET projects. CH thanks support by the Alberta Ingenuity Fund.

References

Barber, G.G., R. Galley, M.G. Asplin, R. De Abreu, K.-A. Warner, M. Pućko, M. Gupta, S. Prinsenberg, and S. Julien (2009), Perennial pack ice in the southern Beaufort Sea was not as it appeared in the summer of 2009, *Geophys. Res. Lett., 36*, L24501, doi:10.1029/2009GL041434.

Giles, K. A., S. W. Laxon, D. J. Wingham, D. W. Wallis, W. B. Krabill, C. J. Leuschen, D. McAdoo, S. S. Manizade, and R. K. Raney (2007), Combined airborne laser and radar altimeter measurements over the Fram Strait in May 2002, *Remote Sens. Environ.*, *111*, 182 – 194, doi:10.1016/j.rse.2007.02.037.

Giles, K. A., S. W. Laxon, and A. L. Ridout (2008), Circumpolar thinning of Arctic sea ice following the 2007 record ice extent minimum, Geophys. Res. Lett., 35, L22502, doi:10.1029/2008GL035710.

Haas, C., and H. Eicken (2001), Interannual variability of summer sea ice thickness in the Siberian and Central Arctic under different atmospheric circulation regimes, *J. Geophys. Res.*, *106 (C3),* 4449-4462.

Haas, C., and P. Jochmann (2003), Continuous EM and ULS thickness profiling in support of ice force measurements, in *Proceedings of the 17th International Conference on Port and Ocean Engineering under Arctic Conditions, POAC ´03, Trondheim, Norway*, edited by S. Loeset, B. Bonnemaire, and M. Bjerkas, *2*, pp. 849-856, Department of Civil and Transport Engineering, Norwegian University of Science and Technology NTNU, Trondheim, Norway.

Haas, C., S. Hendricks, M. Doble (2006), Comparison of the sea ice thickness distribution in the Lincoln Sea and adjacent Arctic Ocean in 2004 and 2005, *Ann.Glaciology*, *44*, 247-252.

Haas, C., A. Pfaffling, S. Hendricks, L. Rabenstein, J. -L. Etienne, and I. Rigor (2008), Reduced ice thickness in Arctic Transpolar Drift favors rapid ice retreat, *Geophys. Res. Lett., 35*, L17501, doi:10.1029/2008GL034457.

Haas, C., J. Lobach, S. Hendricks, L. Rabenstein, and A. Pfaffling (2009), Helicopter-borne measurements of sea ice thickness, using a small and lightweight, digital EM system, *J. Appl. Geoph., 67(3)*, 234–241, 2009, doi:10.1016/j.jappgeo.2008.05.005.

Holland, M. M., C. M. Bitz, and B. Tremblay (2006), Future abrupt reductions in the summer Arctic sea ice, *Geophys. Res. Lett., 33*, L23503, doi:10.1029/2006GL028024.

Hvidegaard, S. M., and R. Forsberg (2002), Sea-ice thickness from airborne laser altimetry over the Arctic Ocean north of Greenland, *Geophys. Res. Lett., 29(20),* 1952, doi:10.1029/2001GL014474.

Kovacs, A., N. C. Valleau, and J. S. Holladay (1987), Airborne electromagnetic sounding of sea-ice thickness and subice bathymetry, *Cold Regions Sci. and Tech., 14*, 289–311.

Kwok, R., and G. F. Cunningham (2008), ICESat over Arctic sea ice: Estimation of snow depth and ice thickness, *J. Geophys. Res., 113*, C08010, doi:10.1029/2008JC004753.

Kwok, R., G. F. Cunningham, M. Wensnahan, I. Rigor, H. J. Zwally, and D. Yi (2009), Thinning and volume loss of the Arctic Ocean sea ice cover: 2003– 2008, *J. Geophys. Res., 114*, C07005, doi:10.1029/2009JC005312.

Lindsay, R., and J. Zhang (2005), The thinning of Arctic sea ice, 1988–2003: Have we passed a tipping point?, *J. Climate, 18*, 4879–4894.

Maslanik, J. A., C. Fowler, J. Stroeve, S. Drobot, J. Zwally, D. Yi, and W. Emery (2007), A younger, thinner Arctic ice cover: Increased potential for rapid, extensive sea-ice loss, *Geophys. Res. Lett., 34*, L24501, doi:10.1029/2007GL032043.

Nghiem, S. V., I. G. Rigor, D. K. Perovich, P. Clemente-Colon, J. W. Weatherly, and G. Neumann (2007), Rapid reduction of Arctic perennial sea ice, *Geophys. Res. Lett., 34*, L19504, doi:10.1029/2007GL031138.

Overland, J., H. Eicken, W. Meier, and H. Wiggins (2009), International Arctic sea ice monitoring program continues into second summer, *Eos, Transact., 90(37)*, 321-322.

Perovich, D. K., J. A. Richter-Menge, K. F. Jones, and B. Light (2008), Sunlight, water, and ice: Extreme Arctic sea ice melt during the summer of 2007, *Geophys. Res. Lett., 35*, L11501, doi:10.1029/2008GL034007.

Pfaffling, A., C. Haas, and J. Reid (2007), A direct helicopter EM sea ice thickness inversion, assessed with synthetic and field data, *Geophysics, 72*, F127-F137.

Reid, J. E., A. Pfaffling, J. Vrbancich (2006), Airborne electromagnetic footprints in 1D earths, *Geophysics, 71(2),* G63-G72, doi:10.1190/1.2187756.

Rothrock, D. A., and M. Wensnahan (2007), The accuracy of sea-ice drafts measured from U.S. Navy submarines, *J. Atmos. Oceanic Technol., 24*, 1936– 1949, doi:10.1175/JTECH2097.1.

Wadhams, P. and N.R. Davis (2001), Arctic sea-ice morphological characteristics in summer 1996, *Ann. Glaciol., 33*, 165-170.

Table 1: Mean and modal thicknesses for flights shown in Figure 1. Individual flights were split into sections of 50 to 100 km length as appropriate to show regional thickness gradients, and are sorted from South to North for each flight. Modal thicknesses are given for predominant modes of new (N), first-year (FY), second-year (SY), and multiyear ice (MY). Classification of ice types is based on a subjective evaluation of the obtained ice thickness distributions and knowledge about ice regimes and age from the scatterometer data in Figure 1.

Table 1:

Flight No.	Date	Length (km)	Latitude (°N), Longitude (°E)[a]	Mean thickness (m)	Standard deviation (m)	Modal thickness (m)[b]
1	April 6	227	81.18, 11.17	1.88	1.03	0.5N, 1.0FY, 2.3SY
			82.25, 9.08	2.36	0.99	0.8N, 2.5SY
2	April 5	143	80.57, 0.74	1.88	1.11	0.4N, 2.2SY
			81.02, -3.41	2.78	1.34	0.7N, 1.6FY, 2.5SY
3	April 9	115	82.62, -58.11	4.41	1.92	2.0FY, 3.1MY
			82.88, -53.56	5.17	2.00	1.9FY, 3.8MY
4	April 10	569	83.23, -63.36	5.66	2.53	4.4 MY
			84.52, -65.62	5.32	2.28	3.2MY
			85.5, -68.63	4.32	1.65	1.6FY, 3.1MY
			86.45, -73.24	3.7	1.35	2.7MY
			87.76, -87.90	3.36	1.32	1.6FY, 2.7MY
5	April 11	357	82.98, -81.06	5.91	2.81	1.8FY, 4.4MY
			83.16, -71.42	6.06	2.71	4.5MY
			82.83, -62.52	5.59	2.38	2.0FY, 3.9MY
6	April 16	426	72.48, -128.67	3.08	1.79	0.2N, 1.1N, 2.0FY, 3.2MY
			72.93, -131.80	3.27	1.88	0.5N, 1.1N, 2.1FY, 3.4MY
			73.37, -135.00	3.10	1.28	0.4N, 0.7N, 2.2SY, 3.0MY
			73.83, -138.29	2.33	1.17	0.6N, 2.3FY
7	April 24	22	72.53, -142.62	1.69	1.11	0.1N, 1.7FY
8	April 26	291	72.22, -158.51	1.94	0.94	0.3N, 1.7FY
			73.31, -161.71	2.02	0.84	1.7FY
9	April 25	262	71.4, -162.37	1.88	1.41	0.1N, 1.6FY
			72.14, -165.45	2.67	1.63	0.2N, 1.5FY

[a] Center location of flight section; negative values represent western longitudes.

[b] Calculated for a bin width of 0.1 m.

Table 2: Ice thickness measurements obtained close to the North Pole, in the Lincoln Sea north of Ellesmere Island, and in the Chukchi Sea in 2009 and in previous years. See Figure 1 and 3 for approximate locations and latitudinal extent of surveys.

Region	Year/Month	Mean thickness (m)	Standard deviation (m)	Modal thickness (m)[a]
North Pole	2007/April[b]	3.55	1.59	2.4SY
87.2-88.3°N, 50-100°W	2009/April	3.36	1.32	2.8SY
Lincoln Sea	2004/May[c]	4.78	2.29	4.0MY
83-84°N, 62-68°W	2005/May[c]	5.30	2.49	4.4MY
	2006/May	5.44	2.70	4.4MY
	2008/May	4.37	1.95	3.2MY
	2009April	5.78	2.59	4.3MY
Chukchi Sea	2007/April	2.56	1.67	1.6FY, 2.8MY
71.5-72.5°N, 152-159°W	2008/April	1.81	1.28	1.2N, 1.8FY, 2.6MY
	2009/April	1.95	1.01	1.8FY

[a] Calculated for a bin width of 0.2 m.

[b] From Haas et al. (2008)

[c] From Haas et al. (2006)

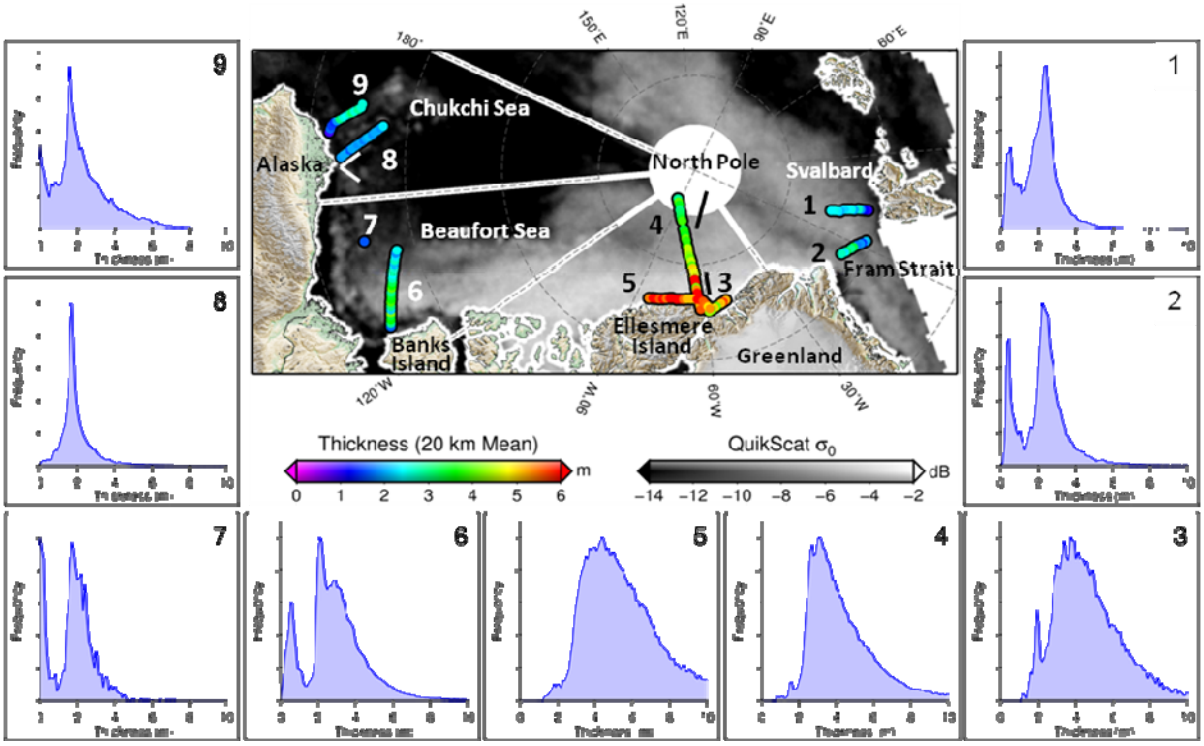

Figure 1: Map of the Arctic Ocean showing ice thickness surveys from April 2009. Colors indicate mean thickness of 20 km flight sections. Grey shades represent sea-ice HH-polarized radar backscatter obtained from the QuikSCAT satellite scatterometer. Sectors indicate different radar acquisition dates within ±1 day of respective thickness surveys. Histograms show ice thickness distributions of all nine flights. Flight numbers are indicated in histograms and on map. Short, bold black and white lines in vicinity of flights 4 and 8 show tracks of surveys in previous years.

Figure 2: Refuelling the BT-67 (“Polar 5”) at Alert, Nunavut, Canada, with the EM Bird cradled between the landing gear under the fuselage.

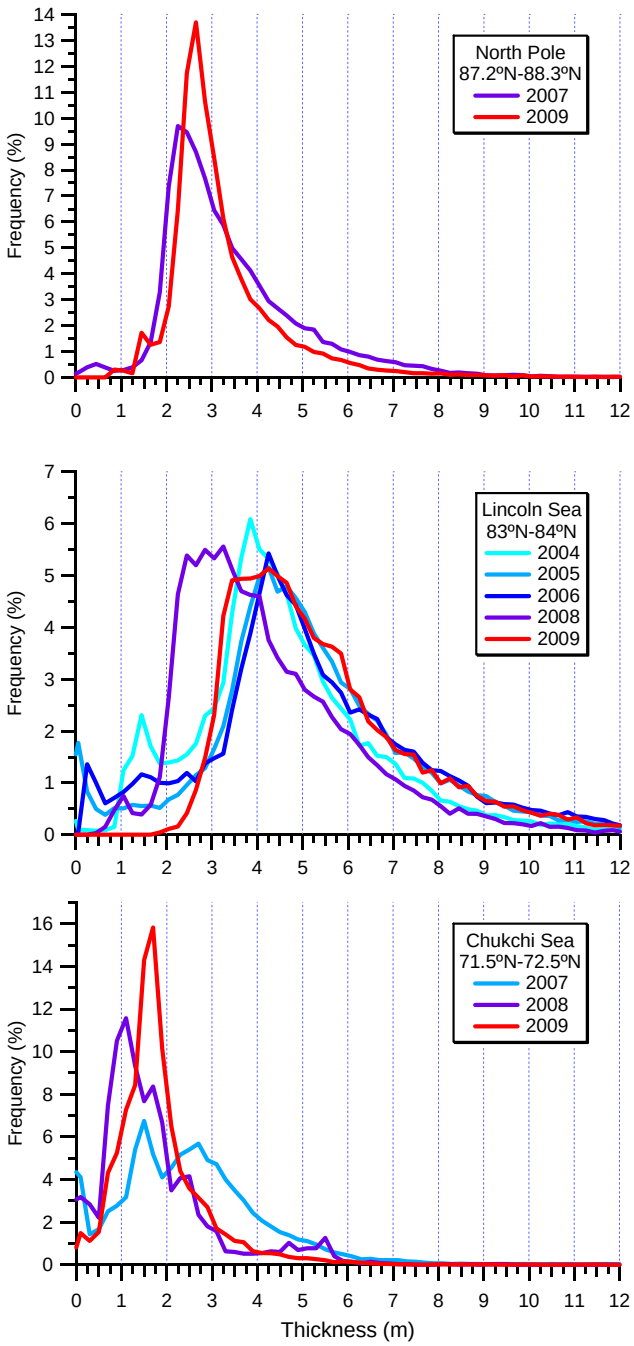

Figure 3: Comparison of ice thickness distributions obtained in different years close to the North Pole (top; 2007 data from Haas et al., 2008), in the Lincoln Sea north of Ellesmere Island (center; 2004 and 2005 data from Haas et al., 2006), and in the Chukchi Sea (bottom). Bin width 0.2 m. Results are summarized in Table 2.